Control of Ion Species and Energy in High-Flux Helicon-Wave-Excited Plasma Using Ar/N_2 Gas Mixtures

Tianyuan Huang, Chenggang Jin, Yan Yang, Xuemei Wu, Lanjian Zhuge, Qinhua Wang, and Hantao Ji

***Abstract*— The atomic nitrogen (N) ion flux and impacting ion energy are the two important parameters, which influence the performance of production of plasma nitridation applications such as N-doped graphene. In this paper, a novel method is described to control the flux and ion energy of atomic N ion (N^+) and molecular N_2 ion (N_2^+) using a helicon-wave-excited plasma (HWP) with Ar/N_2 gas mixtures. It shows that by varying the flow-rate ratio of $N_2/(N_2 + Ar)$ (α), the ratio of $[N^+]/[N_2^+]$ (β) can be controlled obviously, and β could be increased up to 1.2 at $\alpha = 0.5$, which is much higher than that in pure N_2 HWP discharge ($\beta \sim 0.2$). The maximum density and flux of atomic N^+ are obtained, which are 2.5×10^{18} m^{-3} and 8.6×10^{21} $m^{-2}s^{-1}$, respectively. The results show that the addition of Ar into N_2 plasma can be employed to remarkably increase the $[N^+]/[N_2^+]$ due to electron-impact ionization involving the metastable state of Ar. The N^+ ion beams are formed with a speed near to Mach 3, and the ion-beam energy is increased from 30 to 50 eV with increasing α to 0.75.**

***Index Terms*— Helicon-wave-excited plasma (HWP), high-flux atomic nitrogen ion, ion energy distributions.**

Manuscript received October 18, 2017; revised January 29, 2018; accepted February 20, 2018. Date of publication March 26, 2018; date of current version April 10, 2018. This work was supported in part by the National Natural Science Foundation of China under Grant 11505123, Grant 11435009, Grant 11375126, in part by the National Magnetic Confinement Fusion Science Program of China under Contract 2014GB106005, and in part by the Priority Academic Program under Grant 156455. The review of this paper was arranged by Senior Editor F. Taccogna. *(Corresponding author: Chenggang Jin.)*

T. Huang, Y. Yang, X. Wu, and Q. Wang are with the College of Physics, Optoelectronics and Energy & Collaborative Innovation Center, Suzhou Nano Science and Technology, Soochow University, Suzhou 215006, China, and with the Key Laboratory of Advanced Optical Manufacturing Technologies of Jiangsu Province, Soochow University, Suzhou 215006, China, and also with the Key Laboratory of Modern Optical Technologies of Education Ministry of China, Soochow University, Suzhou 215006, China.

C. Jin is with the College of Physics, Optoelectronics and Energy & Collaborative Innovation Center, Suzhou Nano Science and Technology, Soochow University, Suzhou 215006, China, and with the Key Laboratory of Advanced Optical Manufacturing Technologies of Jiangsu Province, Soochow University, Suzhou 215006, China, and with the Key Laboratory of Modern Optical Technologies of Education Ministry of China, Soochow University, Suzhou 215006, China, and also with the State Key Laboratory for Strength and Vibration of Mechanical Structures, Xi'an Jiaotong University, Xi'an 710049, China (e-mail: cgjin@suda.edu.cn).

L. Zhuge is with the Analysis and Testing Center, Soochow University, Suzhou 215123, China.

H. Ji is with the Princeton Plasma Physics Laboratory, Princeton University, Princeton, NJ 08543 USA.

Color versions of one or more of the figures in this paper are available online at http://ieeexplore.ieee.org.

Digital Object Identifier 10.1109/TPS.2018.2812863

I. Introduction

NITROGEN (N) plasmas have been extensively used in a variety of industrial applications such as reactive synthesis of thin film nitridation [1], [2] and surface modification of different materials [3], [4]. These applications are based on dedicated knowledge of plasma chemistry, which demands a precise control of atomic N densities by changing plasma parameters. The atomic N plays a dominant role in the processing of nitridation due to its strong chemical activity, which is associated with the adsorption/diffusion on the material surface. Meanwhile, atomic N can be efficiently incorporated on the surfaces of almost all metals [5]. However, active molecular N_2 (including ionic species) is usually unreactive on the material surface because it is deexcited by a resonant transition below several angstroms of the surface [6]. Recently, low-damage plasma-based (or ion irradiation-based) methods have been used to prepare N-doped graphene, which is considered as a promising material in the field of field-effect transistors [7], lithium batteries [8], fuel cells [9], and supercapacitors [10]. N ion implantation have been investigated as a method for substitutional doping layered graphene showing that N^+ ion energy plays an important role in doping fraction and direct knock-ON/reaction-based vacancy formation [11]. Also, a straightforward mean using direct atomic N^+ implantation and subsequent stabilization at temperatures above 1300 K is reported to produce high-quality N-doped graphene on SiC (0001) [12]. However, due to the difficulty in developing N_2 plasma with a mainly atomic N^+ contribution, the relation between atomic N^+ and the quality of N-doped graphene has not been fully interpreted. Even so, many researchers believe that functionalization using high-density atomic N^+ is necessary to optimize the N-doped graphene property. On the N-doped graphene functionalization applications [11], there is an increasing interest in tuning the ion energy of impinging N^+, which plays a crucial role in surface reactions.

In a pure N_2 plasma discharge, the dissociation degree is low due to the strong N-N bonding (9.76 eV) [13]. In order to increase the dissociation degree, some inert gas (such as Ar) is mixed and different Ar/N_2 plasmas are investigated. For example, a maximum dissociation rate of 10% is observed in low pressure inductively coupled Ar/N_2 plasma [14]. A maximum dissociation of N_2 is obtained in N_2–50% Ar plasma gas mixture in a hollow cathode remote-type RF

0093-3813 © 2018 IEEE. Personal use is permitted, but republication/redistribution requires IEEE permission.
See http://www.ieee.org/publications_standards/publications/rights/index.html for more information.

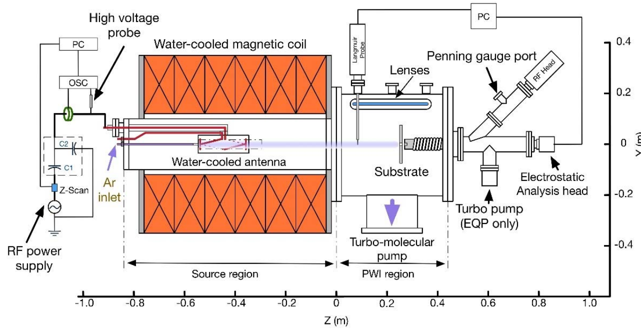

Fig. 1. Schematic of the HMHX setup and the diagnostic system.

discharge system [15]. Energy spectra and mass of ions in Ar/N_2 ECR plasma are investigated using an EQP analyzer and OES [16]. Ar/N_2 plasmas (plasma densities in the range of 10^9–10^{11} cm^{-3}) generated by 2-keV electron beam in a low-pressure background (∼25 mtorr) is characterized using OES [17]. For plasma nitridation (PN), it has been shown that the high N-doping concentration in the modified layer improves with increasing density and energy of atomic N^+ in the plasma. Therefore, high atomic N concentration can be achieved in a short period of time, making the PN processing suitable for high-volume industry manufacturing.

Helicon-wave-excited plasma [18] (HWP) source has attracted a lot of attention due to high electron density (n_e: 10^{17}–10^{20} m^{-3}) and high ionization ratio (∼100%), which can be obtained at low working pressure, making high dissociation degree of molecular N_2 possible. The atomic N species are predominantly produced by the electron-impact processes such as the dissociative collisions between the electron and the molecular N_2^+ (Coulomb collision) or between the electron and the molecular N_2 and these processes strongly depend on the n_e.

In this paper, ion density ratio $[N^+]/[N_2^+]$ are controlled and investigated in HWP with Ar/N_2 gas mixtures by tuning of the gas flow rates of both Ar and N_2 using mass-flow controllers (MFCs). The effect of Ar dilution on the dissociation of molecular N_2 in Ar/N_2 HWP has been evaluated, by measuring the electron energy probability functions (EEPFs) and investigating various plasma parameters as a function of the flow-rate ratio of $N_2/(N_2 + Ar)$ (α), at the relatively low pressures (2×10^{-2} Pa) and high magnetic field (1300G). Much higher atomic N^+ ion flux up to 8.6×10^{21} $m^{-2}s^{-1}$ is achieved with varying α, which opens up new avenues to PN applications.

II. Experimental Setup

The preliminary results on the control of reactive N_2 species are achieved in the high density, steady state, HWP source high magnetic field helicon experiment (HMHX) [19], as shown in Fig. 1. Plasmas are ignited and heated at a low pressure (2×10^{-2} Pa) by a radio frequency (RF, 13.56 MHz) power source, through an internal right helical antenna (50 mm in diameter by 180 mm long). Before the HWP operation, the vacuum chamber is pumped to $<5\times10^{-5}$ Pa by a pumping system consisting of a mechanical pump and a turbo molecular pump. During the operation, the flow rates of Ar and N_2 are controlled by two MFC, respectively, to vary the mixing proportion, and the total gas flow rate is fixed at 20 sccm. The α is varied from 0% (N_2:Ar = 0:20) to 100%, while the RF power is 1500 W, and the magnetic field is 1300 G.

A passively compensated Langmuir probe (Hiden Analytical Limited, ESPION) is positioned 170-mm downstream of the source chamber interface (refer to Fig. 1) for the measurement of the EEPFs and other plasma parameters (including plasma density n_e, effective electron temperature T_e, and plasma potential V_p). The EEPFs play a key role in HWP characterization, which help understand the physical and chemical behavior, which are obtained from the following formula [20]:

$$g(\varepsilon) = \frac{2m_e}{e^2 A}\left(\frac{2\varepsilon}{m_e}\right)^{1/2}\frac{d^2 I}{dV^2} \tag{1}$$

where m_e is the electron mass, e is the electron charge, and A is the physical collecting area of the probe. n_e and T_e are determined as corresponding integrals of the EEPFs from the following formulas:

$$n_e = \int_0^\infty \varepsilon^{1/2} g(\varepsilon) d\varepsilon \tag{2}$$

$$T_e = \frac{2}{3n_e}\int_0^\infty \varepsilon^{3/2} g(\varepsilon) d\varepsilon. \tag{3}$$

A Hiden electrostatic quadrupole plasma (EQP) mass spectrometer analyzer is directly connected to the plasma-material interaction chamber for the measurement of the ion information of the mass and energy spectra. The mass spectrometer is worked in "residual gas analyzer" mode. The 70-eV electron-impact mass spectra are obtained with the plasma on and with the plasma OFF. In each condition, spectra between 10 and 40 amu are obtained and averaged. The dissociation degree D is then calculated using the following equation:

$$D = 1 - \frac{I_{N2_ON}}{I_{N2_OFF}}\frac{I_{Ar_OFF}}{I_{Ar_ON}} \tag{4}$$

where I_{N2_OFF} and I_{N2_ON} are the intensities of the N_2 peak (28 amu) with the plasma OFF and ON, respectively, and I_{Ar_OFF} and I_{Ar_ON} are the intensities of the Ar peak (40 amu) with plasma OFF and ON, respectively.

III. Results and Discussion

A. Dissociation Degree

Fig. 2 shows the measured plasma parameters, including the molecular N_2 dissociation degree $[N]/[N_2]$ [D in (4)] and the ion density ratio of $[N^+]/[N_2^+]$ by varying α. The T_e and V_p increase almost linearly from 3.2 to 6.9 eV and from 11 to 24 V with increasing α, respectively. The n_e is increased up to 5.7×10^{19} m^{-3} with increasing α, followed by a sharp decreasing with $\alpha > 0.5$, as shown in Fig. 2(a) and (b). Fig. 2(c) shows that the D and the ion density ratio of $[N^+]/[N_2^+]$ increase in a similar way to n_e. In any case, it is observed that the dissociation degree D is enhanced when a pure N_2 HWP is transited to an Ar-rich gas mixture HWP.

The enhanced factor of the dissociation degree could be calculated as the ratio of the maximum D obtained from the Ar/N_2 mixture over the $D$from pure N_2. The D starts

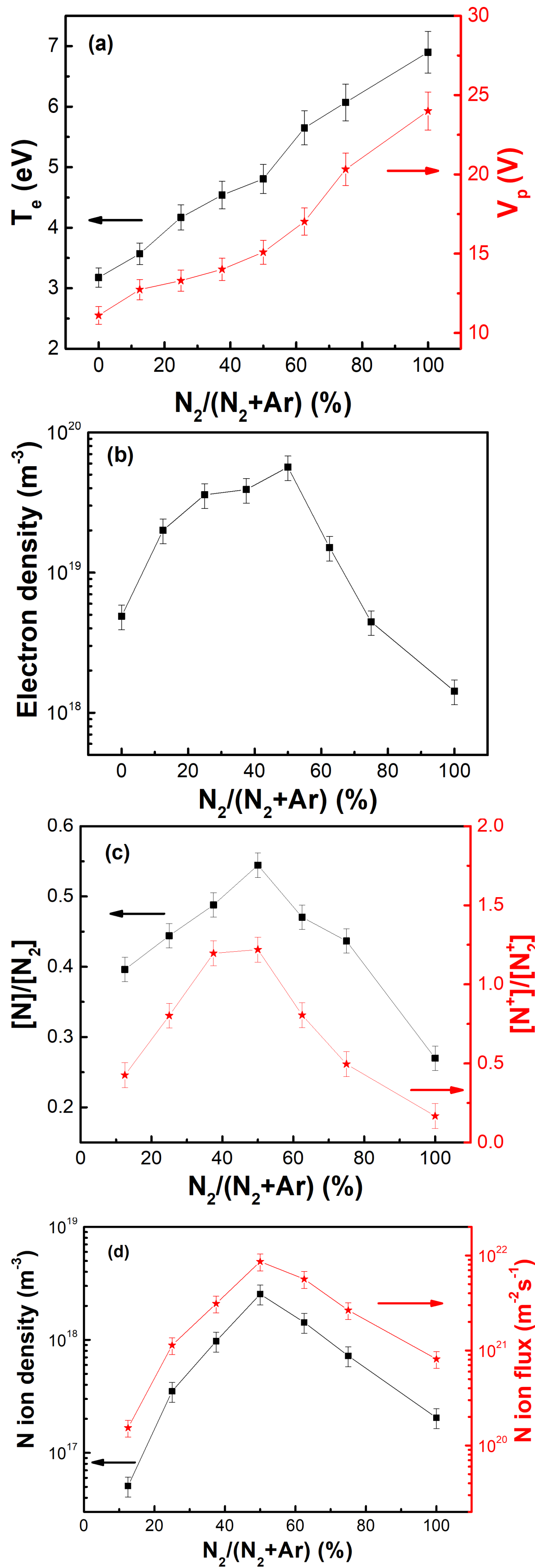

Fig. 2. Measured plasma parameters. (a) T_e (black filled squares) and V_p (red filled pentagons). (b) n_e (black filled squares). (c) Molecular N_2 dissociation level $[N]/[N_2]$ (black filled squares) and ion density ratio of $[N^+]/[N_2^+]$ (red filled pentagons). (d) N^+ density and N^+ flux as a function of α. The RF power was 1500 W, and the mixed gas flow rate was 20 sccm.

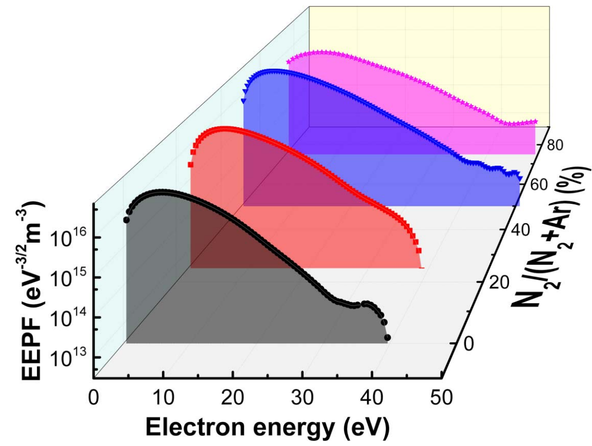

Fig. 3. Measured EEPFs as a function of α. The RF power was 1500 W, and the mixed gas flow rate was 20 sccm.

from 27% (no Ar, $\alpha = 0$) and achieves a maximum of 55% ($\alpha = 0.5$).

Therefore, the dissociation enhancement factor is nearly 2, which indicates that the addition of Ar into N_2 HWP is an efficient method to improve the total ionization rate as well as the $[N^+]/[N_2^+]$. Moreover, the increase of atomic N^+ production is also particularly large. In fact, at α of 0.5, the flux of N^+ is 1.22 times larger than that of N_2^+. It suggests that both D and the $[N^+]/[N_2^+]$ are strong functions of n_e rather than T_e in N_2+Ar mixture HWP. The maximum density and flux of N^+ are 2.5×10^{18} m^{-3} and 8.6×10^{21} $m^{-2}s^{-1}$ at $\alpha = 0.5$, respectively, as shown in Fig. 2(d).

Theoretical analysis results of Ar/N_2 discharge at a frequency of 2.45 GHz show that an increment of Ar proportion in mixture gas bring about an enhancement of the high-energy tail of the EEPFs, which in turn results in higher dissociation degrees of N_2 [21]. As illustrated in Fig. 3, the measured EEPFs in HWP are bi-Maxwellian distribution at the $\alpha > 0.5$. As the α increases, the electron energy loss due to resonant vibrational excitation of N_2 begins to deplete the electrons above 2–3 eV. The bi-Maxwellian distribution in pure N_2 owing to collision less heating of electrons can essentially be attributable to the deep penetration of E–M fields into the HWP, which is a feature of nonlocal electron kinetics at low pressure [22], [23]. The EEPFs develop into a Maxwellian distribution with increasing Ar concentration ($\alpha \leq 0.5$) in the plasma discharge. This revolution of the EEPFs profiles may be related to modifications in energy transport mechanism in the HWP. Furthermore, it can be observed that a steeper slope of the tail temperature (T_e in the high-energy range) at $\alpha \leq 0.5$, which indicates a depletion of high-energy electrons. This can be related to the electron energy "redistribution" in which high-energy electrons transport their energy to low-energy electrons and ionization processing. Therefore, it can be seen that the EEPFs can be tailored by inert Ar mixing. The enhanced ionization rate is because of the metastable atomic Ar (Ar_m^*) reacts with molecular N_2 of the ground state with adding a small amount of Ar into N_2 HWP discharge

$$Ar_m^* + N_2 \rightarrow Ar + N_2^* \quad (5)$$

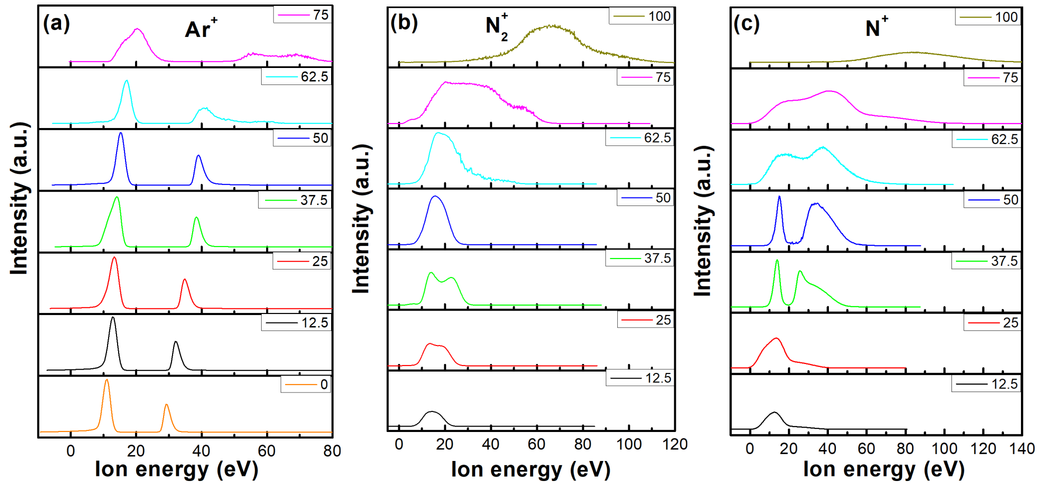

Fig. 4. Normalized ion energy distributions. (a)–(c) Ar^+, N_2^+, and N^+ ions, respectively, as a function of α. The RF power was 1500 W, and the mixed gas flow rate was 20 sccm.

where N_2^* is molecular N_2 of excited states. As N_2^* has the lower threshold ionization energy than that of ground state, N_2^* is easier to be further ionized by electron impact [24]

$$e + N_2^* \rightarrow N_2^+ + 2e \qquad (6)$$

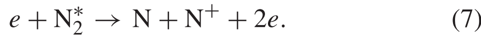

$$e + N_2^* \rightarrow N + N^+ + 2e. \qquad (7)$$

Equations (6) and (7) are the dominant creation processes of N^+, N_2^+, which result in the increase of n_e and N^+ density. Nevertheless, with the further increasing of α, the effect of the two-step ionization would be weakened due to the attenuation of N_2. When the fractions of these two gases turn into closer, the considerable nonresonant charge-exchange reactions result in energy loss when valence electrons occupy different atomic energy levels before and after the collision. Therefore, the n_e and N^+ density become to decline at a certain $N_2/(N_2+Ar)$.

B. Ion Energy Distribution

The Ar/N_2 HWP was further investigated by EQP. The major ion species were Ar^+, N_2^+, and N^+. Fig. 4(a)–(c) gives the ion energy distribution functions (IEDFs) of Ar^+, N_2^+, and N^+ as a function of the α, showing the evolution of peak profiles and the drift of ion energy. Fig. 4(a) shows that the distributed ionization in HWP is responsible for the bimodal energy distribution of Ar^+, which measured at $\alpha < 0.75$. Nevertheless, it can be observed the unimodal energy distribution for N_2^+should be related with diatomic N_2 molecule structures, as shown in Fig. 4(c). In contrast to monatomic molecule, diatomic N_2 molecule contains two atoms and processes rotational and vibration energy levels. In the course of the collisions, the electron-impact excitations of rotational or vibrational energy levels and molecular dissociations can bring about substantial electron energy loss. It inclines to produce N_2^* rather than N_2^+ in local spatial regions. Fig. 4(c) shows that the IEDF of atomic N^+ exhibits two peaks only at α of 0.375 and 0.5, and becomes narrower and shifts toward higher energies as the α is increased from 0.375 to 0.5. The lower energy peak is in response to the local plasma potential ($V_p \sim 15$ V) while the higher energy peak is indicative of ion-beam formation ($V_{\text{beam}} \sim 34$ V) at α of 0.5 [25]. It is an obvious evidence that a double layer (DL) is formed in Ar/N_2 HWP discharge, which accelerates the atomic N^+ ions and creates an ion-beam downstream of the DL. Using an T_e of 4.5 eV for the current conditions determined by the Langmuir probe, the ion-beam velocity and its Mach number could be estimated as [25]

$$v_{\text{beam}} = \sqrt{\frac{2e\left(V_{\text{beam}} - V_p\right)}{M_i}} \sim \sqrt{\frac{8.5kT_e}{M_i}} \sim 2.9c_s. \qquad (8)$$

The Mach number is about 2.9, i.e., it is supersonic. With increasing α, the energy of the ion-beam increases from 30 to 50 eV. As the α is increased, there is an increment in the T_e and potential gradients, which results in larger ion-beam energies for the all α. It indicates that the ion-beam energy can be adjusted by varying the α. These parameters are not expected to change too much at the substrate; therefore, these results exiting here are expected to give an evaluation of plasma chemistry property and ion energy parameter at the substrate.

IV. Conclusion

In this paper, the ion flux and energy of atomic N ion (N^+) and molecular N_2 ion (N_2^+) are controlled by varying the flow-rate ratio of $N_2/(N_2 + Ar)$ (α) in HWP with Ar/N_2 gas mixtures. Due to electron-impact ionization, Ar_m^* are involved, which could remarkably enhance the atomic N^+ and molecular N_2^+ ion creation, especially at the α of 0.5. The ion density ratio is the function of n_e rather than T_e. The maximum density and flux of atomic N^+ are obtained at the α of 0.5, which are 2.5×10^{18} m^{-3} and 8.6×10^{21} m^{-2}s^{-1}, respectively. The N^+ ion beams are formed with a speed near to Mach 3, and the energy of the ion-beam increases from 30 to 50 eV with increasing the α. As the α is increased, there is an increase in the T_e and potential gradients, which result in larger ion-beam energies. Our present experimental results clearly reveal a possible way for generating high atomic N^+ ion flux with impacting ion kinetic energy in the range of 30–50 eV by adjusting the α, and indicate its potential for application in N-doped graphene.

References

[1] S. Dong, M. Watanabe, and R. H. Dauskardt, "Conductive transparent TiN_x/TiO_2 hybrid films deposited on plastics in air using atmospheric plasma processing," *Adv. Funct. Mater.*, vol. 24, no. 20, pp. 3075–3081, Jan. 2014.

[2] S. Calnan *et al.*, "Influence of chemical composition and structure in silicon dielectric materials on passivation of thin crystalline silicon on glass," *Appl. Mater. Interfaces*, vol. 7, no. 34, pp. 19282–19294, Aug. 2015.

[3] M. Rybin *et al.*, "Efficient nitrogen doping of graphene by plasma treatment," *Carbon*, vol. 96, pp. 196–202, Jan. 2016.

[4] C. Yang and Y. J. Yuan, "Investigation on the mechanism of nitrogen plasma modified PDMS bonding with SU-8," *Appl. Surf. Sci.*, vol. 364, pp. 815–821, Feb. 2016.

[5] G. G. Tibbetts, "Electronically activated chemisorption of nitrogen on a copper (100) surface," *J. Chem. Phys.*, vol. 70, no. 8, pp. 3600–3603, Apr. 1979.

[6] H. F. Winters, "Elementary processes at solid surfaces immersed in low pressure plasmas," in *Plasma Chemistry III*. Berlin, Germany: Springer, 1980, pp. 69–125.

[7] D. W. Chang *et al.*, "Nitrogen-doped graphene nanoplatelets from simple solution edge-functionalization for n-type field-effect transistors," *J. Amer. Chem. Soc.*, vol. 135, no. 24, pp. 8981–8988, May 2013.

[8] A. L. M. Reddy *et al.*, "Synthesis of nitrogen-doped graphene films for lithium battery application," *ACS Nano*, vol. 4, no. 11, pp. 6337–6342, Oct. 2010.

[9] L. Qu, Y. Liu, J.-B. Baek, and L. Dai, "Nitrogen-doped graphene as efficient metal-free electrocatalyst for oxygen reduction in fuel cells," *ACS Nano*, vol. 4, no. 3, pp. 1321–1326, Feb. 2010.

[10] H. M. Jeong *et al.*, "Nitrogen-doped graphene for high-performance ultracapacitors and the importance of nitrogen-doped sites at basal planes," *Nano Lett.*, vol. 11, no. 6, pp. 2472–2477, May 2011.

[11] C. D. Cress *et al.*, "Nitrogen-doped graphene and twisted bilayer graphene via hyperthermal ion implantation with depth control," *ACS Nano*, vol. 10, no. 3, pp. 3714–3722, Mar. 2016.

[12] M. Telychko *et al.*, "Achieving high-quality single-atom nitrogen doping of graphene/SiC (0001) by ion implantation and subsequent thermal stabilization," *ACS Nano*, vol. 8, no. 7, pp. 7318–7324, Jun. 2014.

[13] Y. Wang, R. J. van Brunt, and J. K. Olthoff, "Mass spectrometric measurement of molecular dissociation in inductively coupled plasmas," *J. Appl. Phys.*, vol. 83, no. 2, pp. 703–708, Jan. 1998.

[14] T. Czerwiec, F. Greer, and D. B. Graves, "Nitrogen dissociation in a low pressure cylindrical ICP discharge studied by actinometry and mass spectrometry," *J. Phys. D: Appl. Phys.*, vol. 38, no. 24, p. 4278, Dec. 2005.

[15] S. Saloum, M. Naddaf, and B. Alkhaled, "Diagnostics of N2–Ar plasma mixture excited in a 13.56 MHz hollow cathode discharge system: Application to remote plasma treatment of polyamide surface," *J. Phys. D: Appl. Phys.*, vol. 41, no. 4, p. 045205, Feb. 2008.

[16] Y. C. Zhang, X. H. Xie, H. Li, K. Yang, Z. L. Tang, and X. D. Zhu, "Influence of mixture compositions on ion energy distributions in Ar/N_2 electron cyclotron resonance plasma," *Vacuum*, vol. 119, pp. 174–178, Sep. 2015.

[17] E. H. Lock, T. B. Petrova, G. M. Petrov, D. R. Boris, and S. G. Walton, "Electron beam-generated Ar/N_2 plasmas: The effect of nitrogen addition on the brightest argon emission lines," *Phys. Plasmas*, vol. 23, pp. 4040–4048, Apr. 2016.

[18] F. F. Chen, "Plasma ionization by helicon waves," *Plasma Phys. Control. Fusion*, vol. 33, no. 4, p. 339, Apr. 1991.

[19] T. Huang, C. Jin, J. Yu, X. Wu, and L. Zhuge, "High magnetic field helicon plasma discharge for plasma-wall interaction studies," *Sci. China Phys. Mech. Astron.*, vol. 59, no. 4, p. 645201, 2016.

[20] M. A. Lieberman and A. J. Lichtenberg, *Principles of Plasma Discharges and Materials Processing*. Hoboken, NJ, USA: Wiley, 2005.

[21] P. A. Sá and J. Loureiro, "A time-dependent analysis of the nitrogen afterglow in and-Ar microwave discharges," *J. Phys. D: Appl. Phys.*, vol. 30, no. 16, p. 2320, Jan. 1997.

[22] H.-C. Lee, M.-H. Lee, and C.-W. Chung, "Experimental observation of the transition from nonlocal to local electron kinetics in inductively coupled plasmas," *Appl. Phys. Lett.*, vol. 96, no. 4, p. 041503, Jan. 2010.

[23] V. A. Godyak and R. B. Piejak, "Abnormally low electron energy and heating-mode transition in a low-pressure argon RF discharge at 13.56 MHz," *Phys. Rev. Lett.*, vol. 65, no. 8, p. 996, Aug. 1990.

[24] S. Tang *et al.*, "Diagnosis of positive ions from the near-cathode region in a high-voltage pulsed corona discharge N_2 plasma," *J. Vac. Sci. Technol. A, Vac. Surf. Films*, vol. 18, no. 5, pp. 2213–2216, Sep. 2000.

[25] C. S. Corr *et al.*, "Ion beam formation in a low-pressure geometrically expanding argon plasma," *Appl. Phys. Lett.*, vol. 91, no. 24, p. 241501, Dec. 2007.

Tianyuan Huang received the M.Sc. degree in physics from Soochow University, Suzhou, China, in 2014, where he is currently pursuing the Ph.D. degree in plasma physics.

He was a Visiting Researcher at Princeton University, Princeton, NJ, USA, from 2016 to 2017, focused on the carbon arc discharge for synthesis of nanotubes. His current research interests include radio frequency plasma diagnose and plasma material interaction research.

Chenggang Jin received the Ph.D. degree in physics from Soochow University, Suzhou, China, in 2014.

He was a Visiting Researcher at Princeton University, Princeton, NJ, USA, from 2016 to 2017, focused on the two electron emission characteristics of materials. His current research interests include the mechanism of helicon wave plasma and the interaction between plasma and electromagnetic wave.

Yan Yang received the Ph.D. degree in physics from Soochow University, Suzhou, China, in 2017.

Her current research interests include thin film technology and materials, and material characterization.

Xuemei Wu received the B.Sc. degree in physics from Shandong University, Shandong, China, in 1988, the M.Sc. degree in plasma physics from the Institute of plasma physics, Chinese Academy of Sciences, Hefei, china, in 1991, and the Ph.D. degree in physics from Soochow University, Suzhou, China, in 2002.

She was with the Postdoctoral Workstation, Institute of plasma physics, and is involved in the research of new plasma source, physicochemical process of plasma discharge, and preparation of micromaterials and nanomaterials for a long time. She is currently a Professor at Soochow University.

Lanjian Zhuge received the B.Sc. degree in material science and technology from Zhejiang University, Hangzhou, China, in 1986, the M.Sc. degree in physics from Soochow University, Suzhou, China.

He is involved in the research of physicochemical process of plasma discharge, preparation of micromaterials and nanomaterials, and material characterization for a long time. He is currently a Professor at Soochow University.

Qinhua Wang received the Ph.D. degree from the University of Toronto, Toronto, ON, Canada. He is currently the Director with the Jiangsu Key Laboratory for Advanced Optical Manufacturing Technology, Soochow University, Suzhou, China.

He is involved in the research of microstructured optical components designs and manufacturing, laser photothermal radiometry, and optical fiber.

Hantao Ji received the Ph.D. degree in physics from the University of Tokyo, Tokyo, Japan.

He is currently a Professor with the Department of Astrophysical Sciences and a Distinguished Research Fellow with the Princeton Plasma Physics Laboratory, Princeton University, Princeton, NJ, USA. His current research interests include angular momentum transport including magnetorotational instability, magnetic reconnection and plasma-facing components, and plasma-material interactions.